Correlation-Averaging Methods and Kalman Filter-based Parameter Identification for Rotational Inertial Navigation System

Peida Hu, Bingxu Chen,Chenxi Zhang and Qiuping Wu

Abstract— **The attitude accuracy of existing rotational inertial navigation system (RINS) is affected by oscillatory attitude errors caused by the installation errors of rotation axes or inertial sensors. Additional equipment is required to estimate installation errors under dynamic conditions. Methods that use the output of a single RINS to estimate installation errors under dynamic conditions are currently lacking. To address this challenge, this study proposes an installation error estimation method that combines a correlation method, an averaging method, and the Kalman filter. The proposed method adopts a correlation method to increase signal-to-noise ratio, an averaging method to block certain sine signals, and the Kalman filter to identify installation errors in real time. Simulation, turntable, and sea tests were conducted to verify the proposed algorithm. Results show that the estimation accuracy of installation errors is at 10 arcsec levels, which indicates that said errors are estimated accurately using the RINS output initially obtained under dynamic conditions.**

***Index Terms*— correlation method, Kalman filter, self-calibration, installation error, parameter identification, rotational inertial navigation system**

I. Introduction

An Inertial Navigation System (INS) can independently provide navigational information, such as attitude, velocity, and position. INSs are widely applied in consumer electronics, automotive, indoor localization, robot, autonomous underwater vehicle, naval ship, gravimeter, unmanned helicopter system, and aircraft. In autonomous navigations, navigational errors caused by the bias of inertial sensor errors increase with time [1]. To enhance navigational accuracy, a periodic rotation modulation method is utilized to compensate for systematic sensor errors. This method can average gyro bias, asymmetric scale-factor error [2], and accelerometer bias [3]. Thus, long term position, velocity and attitude errors are suppressed effectively, and the navigation accuracy is improved significantly. Nevertheless, the rotation of gimbals or cases causes instantaneous oscillatory type velocity and attitude errors with periods in minutes because of the installation errors of rotation axes [4] or inertial sensors [5]. An oscillatory attitude error can be twice larger than an installation error, and it can seriously affect attitude accuracy. Various installation error models and novel calibration methods have been continually proposed for rotational INS (RINS). Existing installation estimation methods are briefly reviewed as follows.

Under static conditions, a RINS is installed in a motionless base, and its input can be regarded as either constant or zero. Hence, under static conditions, the measurement error can be calculated without external input from other equipment. Wang et al. rotated an inertial measurement unit in one direction along a circular path; they then implemented the same rate in the opposite direction along another circular path [6]. The least squares method has been applied to estimate installation errors by using the average gyroscope output and rotational rate. Song et al. adopted the thin-shell algorithm to calibrate installation errors by using the difference between the gyroscope measurement errors at two opposite rotations [4], given that the gyroscope is sensitive to residual rotation caused by installation errors [7]. In [8], the curve-fitting method was utilized to estimate the first- and second-order terms of angle errors with a specific force. Kang et al. estimated installation errors by applying singular value decomposition (SVD) with a specific force at four positions in a matrix [9]. Wang et al. identified installation errors by employing the average of the north and east velocity errors [10]. In addition, Gao et al. applied the recursive least squares method to calibrate installation errors by using attitude and velocity errors [11]. In a recently published article, installation errors were directly calculated using the attitude matrices obtained before and after rotation [12]. Gao et al. adopted the Kalman filter to estimate installation errors by using velocity and position errors [13]. Wang et al. utilized the extended Kalman filter to calibrate installation errors with attitude and velocity errors [14]. Under dynamic conditions and considering the motion of the ship, RINS is installed on a moving base, and the inertial sensors are sensitive to the motion of the vehicle [15]. Hence, the input of RINS evolves. Accordingly, the external reference provided by other equipment is necessary to calculate measurement errors. In the marine ring laser inertial navigator, Levinson and Majure (1987) employed the Kalman filter to estimate the installation errors of a RINS by performing dockside and at-sea reference velocity measurements [2].

For RINS, once the gyroscope, the accelerometer, attitude, or

This work was supported in part by the National Natural Science Foundation of China under Grant 61603208 and in part by Tsinghua University Initiative Scientific Research Program under Grant 20151080461. Paper no. TII-18-0229. (Corresponding author: Peida Hu.)

The authors are with the Department of Precision Instrument, Tsinghua University, Beijing 100084, China (e-mail: hpd211@mail.tsinghua.edu.cn; chenbx15@mails.tsinghua.edu.cn;zhangchenxi1995@126.com; wuqiuping@mail.tsinghua.edu.cn).

velocity error caused by installation errors is obtained, the installation errors can be accurately estimated using the following algorithms or methods: the least squares method, recursive least squares method, curve-fitting method, thin-shell algorithm, SVD, averaging method, Kalman filter, and extended Kalman filter. The biggest difference among the aforementioned methods lies in the types of measurement errors selected to identify installation errors. We can choose the estimation method according to the precision of available measurement information. However, existing methods have failed to identify installation errors without an external reference provided by another equipment in dynamic condition. However, RINSs are frequently used in autonomous sea navigation [12], that is, under dynamic conditions, in which external references are either difficult to obtain accurately or even unavailable. Estimation methods for installation errors under dynamic conditions by using the output of a single RINS are currently lacking. The difficulty in estimating installation errors utilizing only RINS output is analyzed as follows. The expected estimation accuracy for an installation error is at 10 arcsec level [4] [8]; however, vessel motion causes vehicle attitude to fluctuate by several degrees [16]. Installation errors should be separated from attitude. Consequently, the signal-to-noise ratio (SNR) for identifying installation errors is extremely low, which affects the performance of the estimation method. Furthermore, installation errors may gradually evolve. Therefore, estimation should be performed in real time. However, the estimation of parameters in real time under low SNR is a challenge for RINS. To date, calibrating installation errors under dynamic conditions without an external reference remains infeasible. To overcome the aforementioned limitation, an error estimation method that combines a correlation method, an averaging method, and the Kalman filter is proposed in the current study.

The Kalman filter is widely used in real-time parameter identification [17]; however, this filter cannot address noise in inaccurate statistical parameters and dynamic models. Feng et al. applied a maximization particle filter to estimate the initial parameters for the Kalman filter and to solve its limitations [17]. The particle filter was employed to deal with nonlinear models, whereas the Kalman filter was used to estimate the states of linear Gaussian state-space models [18]. These methods cannot suppress the large disturbance caused by vessel motion. Thus, correlation and averaging methods are utilized to improve SNR.

SNR can be initially increased using the correlation method because a signal has a correlation of zero at a certain period [19]. The output correlation method was adopted to enhance SNR, and the Kalman filter was adopted to detect low-amplitude electroencephalogram spikes, but it failed to distinguish signals with similar frequencies [20]. The known frequencies of an output can be identified by correlating the output with a cosine function of a known frequency [21]. Thus, SNR will increase as noise components decrease, highlighting the components of interest when the attitude is correlated with the rotation angle.

An extended observation time is required to effectively increase low SNR; however, doing so may seriously affect system security [22]. The averaging method was used in [23] to reduce the observation errors of the Kalman filter when industrial wireless sensor networks operate under harsh conditions. The averaging method was also used to suppress high frequency noise of inertial sensors in [24] and to block the sinusoidal disturbances of the integer multiples of a given frequency in [25]. Then, SNR can be further increased by suppressing measurement noise and sinusoidal disturbances, similar to the process for radiation force-based elasticity imaging [26]. Given that correlation and averaging methods have significantly increased SNR according to the frequency-domain features of the attitude, the Kalman filter can be applied to estimate installation errors by combining the average value and the installation error model in time-domain. Thus, not only the large disturbance caused by the vessel motion but also the measurement errors brought by RINS will be considered in our proposed method.

This study proposes a universal installation error estimation method for the RINSs installed in different types of ships, but ship dynamics is neglected here for two reasons. First is that different types of ships have varied ship dynamics models. The second reason is the difficulty of describing ship dynamics. Hence, the installation error estimation method is proposed to estimate installation errors by solely using the attitude provided by RINS without utilizing the model of ship dynamics. Our developed RINS is adopted to verify our proposal.

The rest of this paper is organized as follows. The limitations of the existing installation error estimation method are shown in Section II. The proposed installation error estimation method and its simulation results are reported in Section III. The experimental performance of the proposed method is discussed in Section IV. Finally, the conclusion is presented in Section V.

II. Limitations of Existing Signal Processing

Attitude parameters are defined in terms of three angles, namely, heading, roll, and pitch. The attitude provided by RINS mainly consists of the true attitude of a vehicle caused by ship motion, oscillatory attitude errors caused by installation errors, and low-frequency errors due to sensor errors, as illustrated in Fig. 1 [27]. The installation errors of RINS can be defined as

$$\begin{pmatrix} x_1 & x_2 & x_3 & x_4 \end{pmatrix} = \begin{pmatrix} \alpha_1 \sin\varphi_1 & \alpha_1 \cos\varphi_1 & \alpha_2 \sin\varphi_2 & \alpha_2 \cos\varphi_2 \end{pmatrix} \tag{1}$$

where α_1 and α_2 are the amplitudes and φ_1 and φ_2 are the phases of installation errors. The oscillatory heading $\delta\psi_{\mathrm{m}}$, roll $\delta\phi_{\mathrm{m}}$, and pitch $\delta\theta_{\mathrm{m}}$ errors caused by the installation errors of the developed RINS at time t can then be written as follows [28]:

$$\begin{cases} \delta\psi_{\mathrm{m}} = -x_1 \cos L \cos(\rho(t) - s(t)) - x_2 \cos L \sin(\rho(t) - s(t)) \\ \qquad -x_3 \sin L \sin \rho(t) + x_4 \sin L \cos \rho \\ \delta\phi_{\mathrm{m}} = -x_1 \sin L \cos(\rho(t) - s(t)) - x_2 \sin L \sin(\rho(t) - s(t)) \\ \qquad + x_3 \cos L \sin \rho(t) - x_4 \cos L \cos \rho(t) \\ \delta\theta_{\mathrm{m}} = x_1 \sin(\rho(t) - s(t)) - x_2 \cos(\rho(t) - s(t)) \end{cases} \tag{2}$$

This article has been accepted for publication in a future issue of this journal, but has not been fully edited. Content may change prior to final publication. Citation information: DOI 10.1109/TII.2018.2850756, IEEE Transactions on Industrial Informatics

where $s(t)$ is the angle of the platform with a period of 24 h, $\rho(t)$ is the rotation angle of RINS with a period of 480 s, and L is the local latitude of RINS.

Roll error is analyzed as an example given that heading, roll, and pitch errors exhibit similar error characteristics [29]. The roll provided by RINS can be expressed as

$$\phi = \phi_{\mathrm{p}} + \delta\phi_{\mathrm{m}} + \delta\phi_{\mathrm{g}} + \delta\phi_{\mathrm{n}} \tag{3}$$

where ϕ_{p} is the true roll angle, $\delta\phi_{\mathrm{g}}$ is the low-frequency error with a period of over 12 h [27], and $\delta\phi_{\mathrm{n}}$ is the high-frequency noise of RINS.

Then, ϕ_{p} can be approximated as

$$\phi_{\mathrm{p}} = A\sin(\omega_{\mathrm{y}} t) \tag{4}$$

where A is the amplitude, and ω_{y} is the angular rate of the true roll with a period of 6–10 s.

In accordance with [29], $\delta\phi_{\mathrm{g}}$ can be written as

$$\delta\phi_{\mathrm{g}} = a_0 + a_1\sin(\omega_{\mathrm{e}} t) + a_2\cos(\omega_{\mathrm{e}} t) + a_3\sin(2\omega_{\mathrm{e}} t) + a_4\cos(2\omega_{\mathrm{e}} t) \tag{5}$$

where $(a_0, a_1, a_2, a_3, a_4)^{\mathrm{T}}$ is the unknown constant coefficient vector, and ω_{e} is the inertial angular rate of the Earth.

When an external reference can be obtained, roll error $\delta\phi$ can be calculated by subtracting external roll reference ϕ_{T} from ϕ as follows:

$$\delta\phi = \phi - \phi_{\mathrm{T}}. \tag{6}$$

$\delta\phi$ can then be utilized to identify installation errors using the Kalman filter. However, $\delta\phi$ cannot be derived under a dynamic condition in which an external reference is lacking. Thus, installation errors should be estimated by employing ϕ. The expected estimation accuracy of installation errors is at 10 arcsec level, but the fluctuation of the true attitude is at a level of several degrees, indicating that SNR may be less than 0.001. To demonstrate the disadvantage of the existing method, we select the Kalman filter as an example because this algorithm has been widely adopted in installation error identification recently [13,14,30].

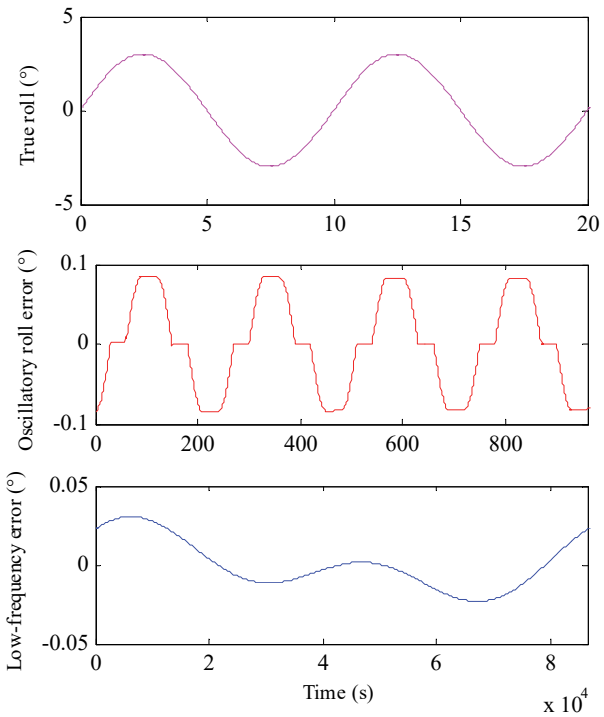

Fig. 1 Attitude provided by RINS

A simulation is conducted to demonstrate the performance of the Kalman filter without external reference. The magnitude and period of the true roll fluctuation are set to 3° and 6 s, respectively. The magnitude and period of low-frequency roll errors are set to 0.05° and over 43200 s, respectively, as depicted in Fig. 1. Oscillatory roll errors are presumably caused by installation errors x_1, x_2, x_3, and x_4, with amplitudes at hundreds of arcsec levels. The Kalman filter is employed to identify the constant installation errors. To evaluate the performance of the installation error estimation method, the absolute percentage error σ is defined as

$$\sigma = \left|\left(\text{Estimation value-True value}\right)/\text{True value}\right| \times 100\%. \tag{7}$$

As shown in Fig. 2, the absolute errors of the estimation values reach 131% after 2 days, which indicates that the filter does not converge even after 2 days.

Therefore, the Kalman filter is unsuitable for calibrating installation errors without an external reference. Similarly, the disturbance caused by vessel motion will also affect the estimation accuracy of other installation error estimation methods. Hence, correlation and averaging methods are used to enhance SNR according to the frequency domain characteristics of the installation errors before applying existing installation error estimation methods.

This article has been accepted for publication in a future issue of this journal, but has not been fully edited. Content may change prior to final publication. Citation information: DOI 10.1109/TII.2018.2850756, IEEE Transactions on Industrial Informatics

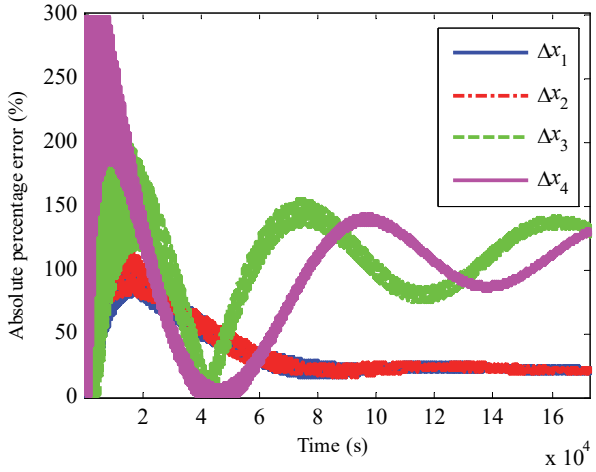

Fig. 2 Absolute percentage errors using the traditional method

III. Installation Error Estimation Method

The proposed installation error estimation method adopts a correlation method to increase SNR, an averaging method to block certain sine signals, and the Kalman filter to identify installation errors. The proposed method is described as follows.

A. Correlation method

On the basis of (2), installation errors can be separated from heading, roll, or pitch. We select roll and pitch to estimate installation errors given that heading errors are divergent with time [27]. Pitch is selected to estimate x_1 and x_2 because oscillatory pitch errors are caused only by x_1 and x_2. Roll is then selected to estimate x_3 and x_4. We use the estimation method of x_3 as an example given that roll and pitch errors demonstrate similar error characteristics. The correlation between roll and rotation angle is utilized to increase SNR, whereas the oscillatory roll error due to installation errors changes with the rotation angle of RINS, as expressed in (2). The correlation between ϕ and $\sin(\rho(t))$ can be written as[31]

$$R_{1s}(t)=\left(\int_0^t \phi \sin\rho(\tau)d\tau\right)/t. \tag{8}$$

When (2–5) are substituted into (8), $R_{1s}(t)$ can be approximated as

$$R_{1s}(t)=\left(r_{1s1}(t)+r_{1s2}(t)+r_{1s3}(t)+r_{1s4}(t)+r_{1s5}(t)\right)/t \tag{9}$$

where

$$\begin{cases} r_{1s1}(t)\approx x_3 t\cos L/2 \\ r_{1s2}(t)\approx -\dfrac{A}{\omega_y}\left[\sin\left(\omega_y\tau\right)\cos\rho(\tau)\right]_0^t \\ r_{1s2}(t)\approx -\dfrac{A}{\omega_y}\left[\sin\left(\omega_y\tau\right)\cos\rho(\tau)\right]_0^t \\ r_{1s3}(t)\approx \dfrac{-1}{\omega_r}\left[\begin{pmatrix} a_0+a_1\sin(\omega_e\tau)+a_2\cos(\omega_e\tau) \\ +a_3\sin(2\omega_e\tau)+a_4\cos(2\omega_e\tau)\end{pmatrix}\cos\rho(\tau)\right]_0^t. \\ r_{1s4}(t)\approx \dfrac{1}{4\omega_r}\begin{bmatrix} x_1\sin L\sin\left(2\rho(\tau)-\omega_e\tau\right) \\ +x_2\sin L\cos\left(2\rho(\tau)-\omega_e\tau\right) \\ -x_3\cos L\cos(2\rho(\tau)) \\ +x_4\cos L\cos(2\rho(\tau))\end{bmatrix}_0^t \\ r_{1s5}(t)\approx \dfrac{1}{2\omega_e}\left[-x_1\sin L\sin\left(\omega_e\tau\right)+x_2\sin L\cos\left(\omega_e\tau\right)\right]_0^t \end{cases} \tag{10}$$

The period and amplitude of each item are listed in Table I.

TABLE I.
ELEMENTS OF THE CORRELATION VALUE

Symbol	Period (s)	Amplitude (arcsec)
$r_{1s1}(t)$	Linear curve	
$r_{1s2}(t)$	6–10	Ten thousand
$r_{1s3}(t)$	480	Several hundreds
$r_{1s4}(t)$	240	Several thousands
$r_{1s5}(t)$	≥ 43200	Several millions

In accordance with (9) and Table I, $\left(r_{1s2}(t)+r_{1s3}(t)+r_{1s4}(t)+r_{1s5}(t)\right)/t$ is decreased to zero and $R_{1s}(t)$ converges to $\left(x_3\cos L\right)/2$ with increased integral time. The correlation values of the true roll, oscillatory roll, and low-frequency errors are presented in Fig. 3 (blue). The correlation value of the oscillatory roll errors converges to $\left(x_3\cos L\right)/2$. The correlation values of the true roll and low-frequency errors are decreased to zero. However, the correlation value contains periodical disturbances in the initial stage. An averaging method is adopted to suppress periodical disturbances and accelerate convergence.

B. Averaging method

An averaging method with a window length of 480 s is adopted because such method can block the sinusoidal disturbances of the integer multiples of a certain frequency. Output signal $\overline{R_{1s}}(t)$ can be written as

$$\overline{R_{1s}}(t)=\left(\int_{t-240}^{t+240} R_{1s}(\tau)d\tau\right)/480. \tag{11}$$

The adopted averaging method traverses the constant component and completely blocks the frequency components of the integer multiples of 1/480 (in Hz). The time delay caused by the averaging method is neglected because the true value of

This article has been accepted for publication in a future issue of this journal, but has not been fully edited. Content may change prior to final publication. Citation information: DOI 10.1109/TII.2018.2850756, IEEE Transactions on Industrial Informatics

x_3 remains constant for several days. $\overline{R_{\text{ls}}(t)}$ can then be expressed as

$$\overline{R_{\text{ls}}(t)} \approx \frac{-x_1 \sin L \sin(\omega_e t)+x_2 \sin L\left(\cos(\omega_e t)-1\right)}{2\omega_e t}+\frac{1}{2}x_3 \cos L . \tag{12}$$

As shown in Fig. 3 (red), the amplitudes of periodical disturbances decreased rapidly during the initial stage.

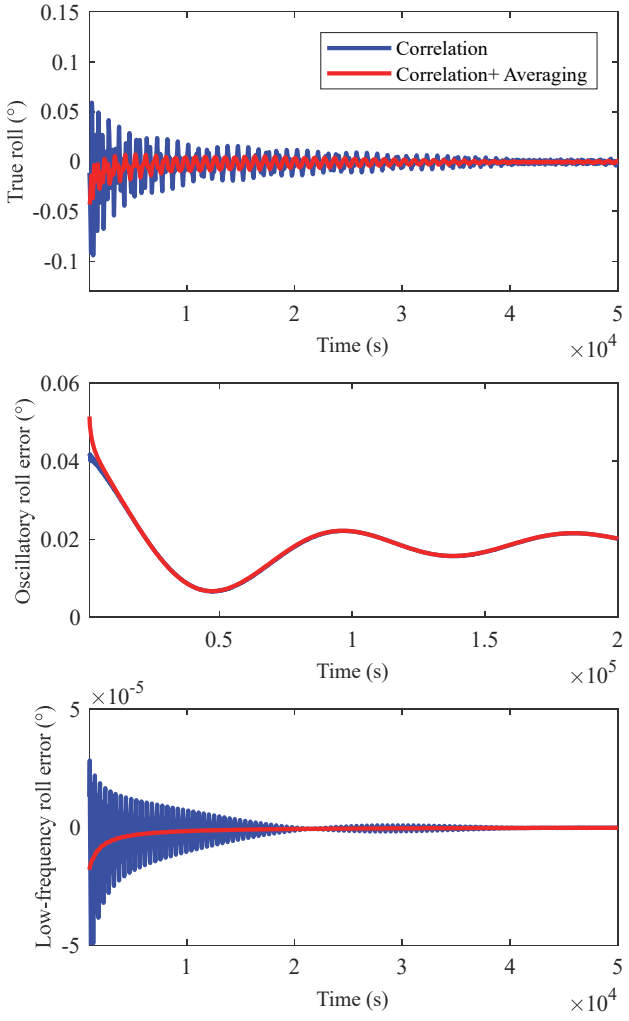

Fig. 3 Correlation values (blue) of the true roll, oscillatory roll, and low-frequency errors; average values (red) of the correlation values

C. Kalman filter

After performing the correlation and averaging methods, $\left(-x_1 \sin L \sin(\omega_e t)+x_2 \sin L\left(\cos(\omega_e t)-1\right)\right)/(2\omega_e t)$ changes gradually after several rotation periods, and then $\overline{R_{\text{ls}}(t)}$ is approximated as

$$\overline{R_{\text{ls}}(t)} \approx x_3\left(\cos L\right)/2+b_1 \sin \omega_e t+b_2 \cos \omega_e t \tag{13}$$

where b_1 and b_2 are the constant coefficients.

The continuous (13) can be discretized as

$$\overline{R_{\text{ls}}(k)} \approx x_3\left(\cos L\right)/2+b_1 \sin\left(k\omega_e T_s\right)+b_2 \cos\left(k\omega_e T_s\right) \tag{14}$$

where k is the discretization step with a sample interval of T_s.

The 3D state variables of the system are expressed as

$$\boldsymbol{\eta}_k=\begin{pmatrix} x_3 & b_1 & b_2 \end{pmatrix}. \tag{15}$$

The observation vector z_k of the system is calculated by

$$z_k=\overline{R_{\text{ls}}(k)} \tag{16}$$

where $\overline{R_{\text{ls}}(k)}$ is the value of $\overline{R_{\text{ls}}(t)}$ at time t_k.

The observation matrix is obtained as follows:

$$\boldsymbol{H}_k=\begin{pmatrix} \cos L/2 & \cos \omega_e t_k & \sin \omega_e t_k \end{pmatrix}. \tag{17}$$

The system state equation is neglected because the Kalman filter estimates constant installation errors. The measurement equation is then obtained as

$$z_{k+1}=\boldsymbol{H}\boldsymbol{\eta}_k^{\mathrm{T}}+W_k \tag{18}$$

where random variables W_k represent state noise.

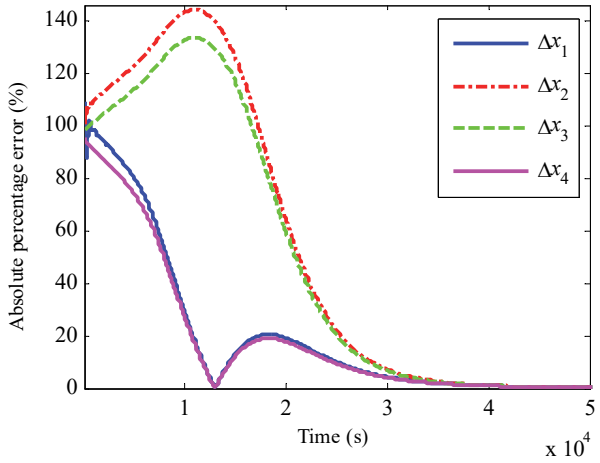

Fig. 4 Absolute percentage errors using the proposed method

The absolute percentage errors of the estimated installation errors are within 0.5% in 45000 s, as illustrated in Fig. 4. A comparison between Figs. 2 and 4 indicates that estimation accuracy is higher in the proposed method than in the traditional method. The run time of the Kalman filter is set to 45000 s according to the simulation result.

IV. Experimental Verification

A. Turntable Test

A turntable test is conducted to verify the proposed method. The three-axis turntable simulates the attitude motion of a vehicle and provides the attitude reference with an attitude accuracy of 10 arcsec (root mean square) [32]. The turntable is installed on a static base. The RINS, which consists of two dual-axis gyroscopes with low drift rates and three pendulous accelerometers mounted on a gimbaled platform, is mounted on the turntable. The accelerometer bias and gyro drift of the RINS are 2×10^{-5} g and 1×10^{-3} °/h, respectively. Before the test, the

This article has been accepted for publication in a future issue of this journal, but has not been fully edited. Content may change prior to final publication. Citation information: DOI 10.1109/TII.2018.2850756, IEEE Transactions on Industrial Informatics

misalignment in angles between the turntable and RINS are measured and compensated for by using a tachymeter and a high-precision electronic level meter. The turntable and RINS output is synchronized using a time-synchronization signal. The installation estimation algorithm is implemented in Microsoft Visual Studio 6.0, and the test is run on a Lenovo T61 with a 2.1 GHz Core2 Duo Intel T8100 processor and 2 GB RAM. The run time of the proposed method is 0.7 ms. The case rotation angles, platform angles, latitude, and attitude of RINS are collected at a sampling period of 1 s. Hence, the practical run time of the installation estimation algorithm is considerably less than the required time of 1 s.

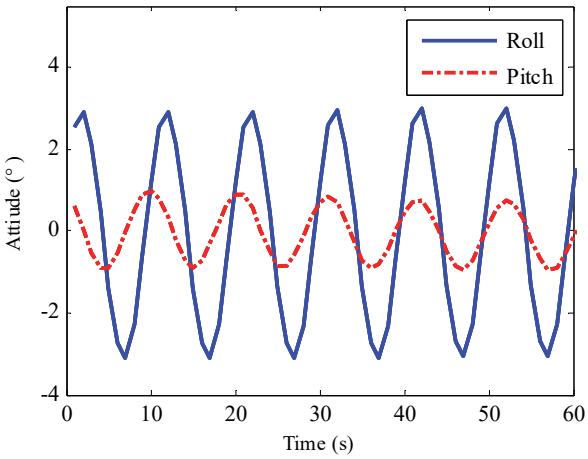

Fig. 5 Roll and pitch values in the turntable test

The amplitudes of roll and pitch are at 3° and 1° levels, respectively, and the periods of roll and pitch are at 10 s level, as illustrated in Fig. 5. The Kalman filter is applied to estimate installation errors using roll and pitch after the turntable starts swaying. The estimated installation errors at 45000 s are assumed as installation error references. Fig. 6 presents the estimated installation errors converging rapidly after 20000 s and then the estimation errors are reduced to 10 arcsec in 4.5×10^4 s. Fig. 7 shows the attitude errors at 350 arcsec levels before the installation errors are calibrated. Fig. 8 displays the attitude errors reduced from 350 arcsec to 10 arcsec, which indicates that the estimation accuracy of the installation errors is at 10 arcsec level. The turntable test results indicate that the proposed installation error estimation method can estimate installation errors accurately under dynamic conditions. Therefore, a sea test is performed to verify the performance of the proposed method at sea.

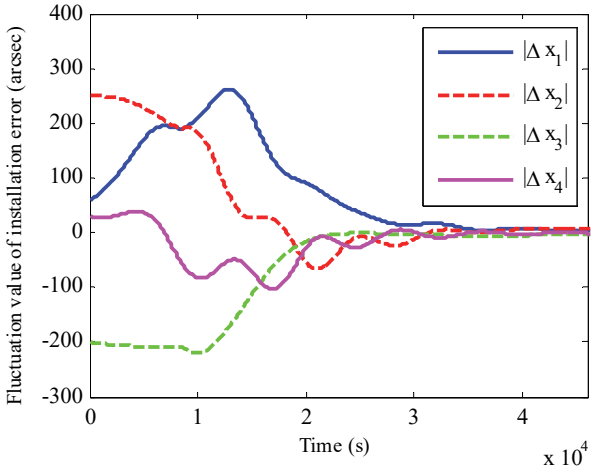

Fig. 6 Fluctuation values of installation errors in the turntable test

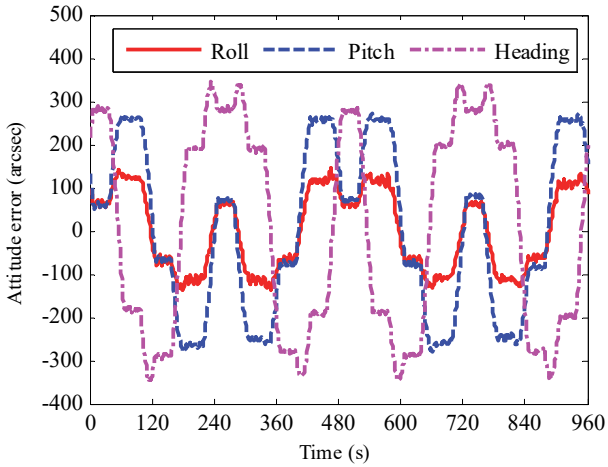

Fig. 7 Atttiude error before calibration

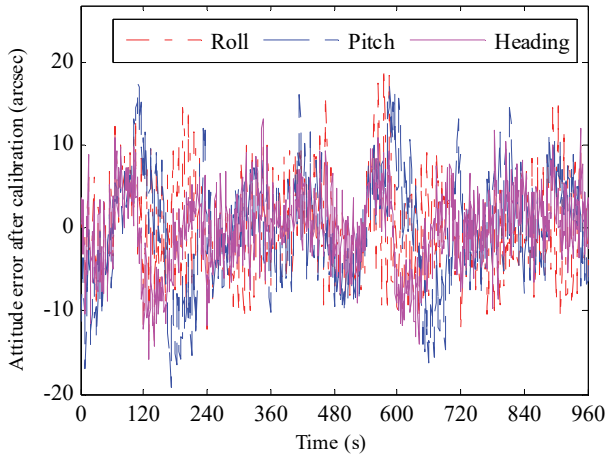

Fig. 8 Atttiude error after calibration

This article has been accepted for publication in a future issue of this journal, but has not been fully edited. Content may change prior to final publication. Citation information: DOI 10.1109/TII.2018.2850756, IEEE Transactions on Industrial Informatics

B. Sea Test

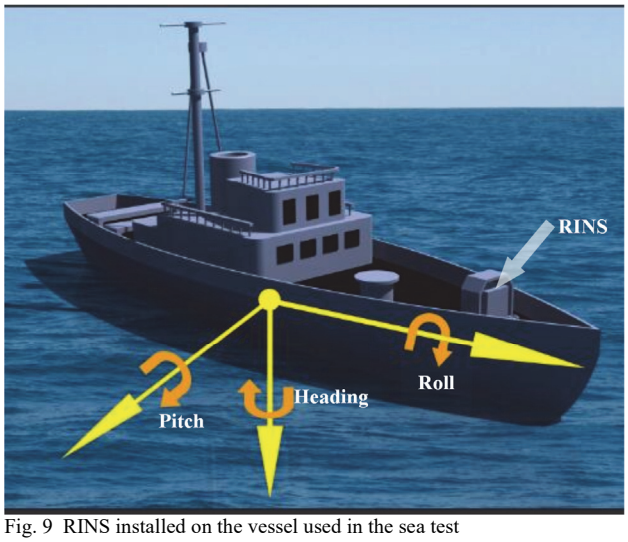

Fig. 9 RINS installed on the vessel used in the sea test

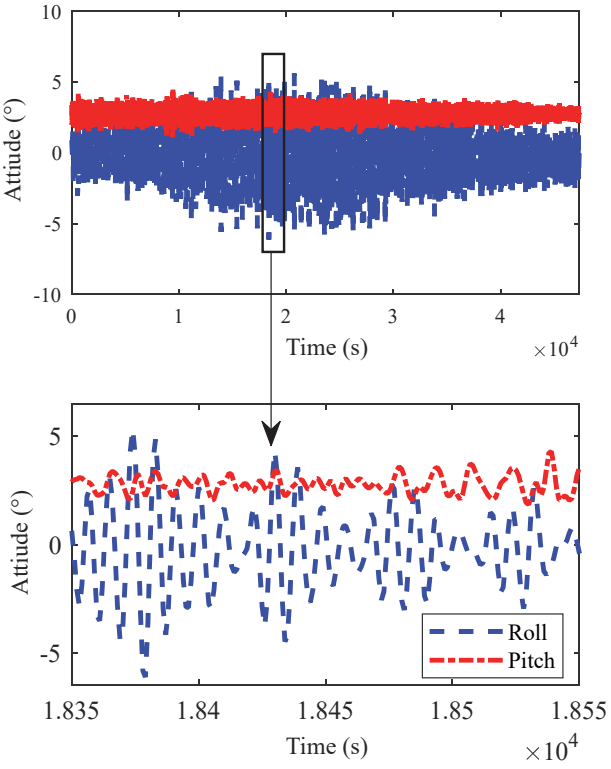

Fig. 10 Roll and pitch values in the sea test

Installation errors are estimated under static conditions before the sea test is conducted and regarded as installation error references, given that a high-accuracy attitude reference is difficult to obtain. The estimated installation error values in the turntable and sea tests differ because the gyroscopes are replaced after the turntable test. The case rotation angle, platform angle, latitude, and attitude of the RINS are also collected at a sampling period of 1 s; hence, the hardware and software configurations used in the turntable test are also adopted in the sea test. The RINS is installed at the front of the vessel, as shown in Fig. 9.

To verify the performance of the proposed method under dynamic conditions, the vessel starts to sail the sea in a low-latitude area. The vessel moves with a forward velocity of 5 m/s. The heading, roll, and pitch rates are 0.5°/s, 3.0°/s, and 0.7°/s, respectively. Motion occurs in the entire installation error estimation process as shown in Fig. 10 (top panel), which lasts 47340 s. The typical amplitudes of roll and pitch are at 6.0° and 1.5° levels, respectively, and the periods of roll and pitch are at 10 s level, as shown in Fig. 10 (bottom panel). The expected estimation accuracy of the installation error is at 10 arcsec level; however, the fluctuation of the roll reaches 6.1°, which indicates that SNR is less than 0.001. The installation error estimation method is initiated when the fluctuation amplitude of the roll is higher than 3°. Estimation errors are calculated by subtracting the estimated installation errors from the installation error references under static conditions. Fig. 11 illustrates that estimation errors are decreased to 10 arcsec within 45000 s, which indicates that the proposed installation error estimation method can accurately estimate installation errors under dynamic conditions. The results of the simulation, turntable test, and sea test indicate that the proposed method can estimate installation errors under dynamic conditions without additional equipment.

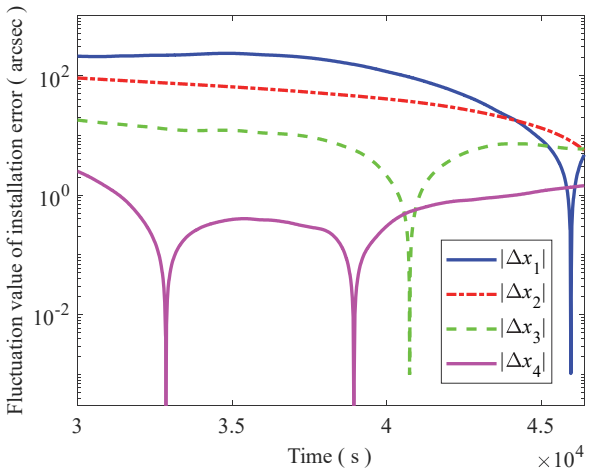

Fig. 11 Fluctuation values of installation errors in the sea test

V. Conclusion

This study aims to resolve the difficulty of estimating installation errors in RINS without external references under dynamic conditions. A method that combines a correlation method, an averaging method, and the Kalman filter is proposed to estimate installation errors by using the attitude provided by a single RINS instead of relying on external references under dynamic conditions, thereby solving the aforementioned limitation. The correlation method suppresses the disturbance caused by the motion of the ship, the averaging method blocks certain periodical disturbances due to rotation,

and the Kalman filter estimates installation errors in real time. The proposed method is specifically designed according to the time- and frequency-domain features of the attitude. Hence, it can suppress large disturbance caused by the vessel motion and measurement error brought out by the RINS. The simulation, turntable, and sea tests demonstrate that the proposed method can estimate installation errors without external references under dynamic conditions. Thus, we successfully addressed the challenge of estimating RINS installation errors under dynamic conditions without any external reference and can solve the oscillatory error estimation problem of the RINS first pointed out by Levinson and Majure in 1987.

We hope that this work will pose a challenge in error parameter identification without external reference and encourage readers to apply the proposed method in various areas. Future works can also apply the proposed method to fault detection, fault location, and parameter calibration under ultralow SNR in industrial fabrication and manufacturing processes, particularly when data are collected over a long period.

REFERENCES

[1]H. Zhao, and Z. Y. Wang, "Motion measurement using inertial sensors, ultrasonic sensors, and magnetometers with extended Kalman filter for data fusion, " IEEE Sensors Journal, vol. 12, no. 5, pp. 943-953, 2012.
[2]E. Levinson, and R. Majure, "Accuracy enhancement techniques applied to the marine ring laser inertial navigator (MARLIN)," Navigation, vol. 34, no. 1, pp. 64-86, 1987.
[3]J. Chen, L Wang, Z.J. Liu, G. H. Su, and G. J. Cao, " Calibration and data processing technology of gyroscope in dual axis rotational inertial navigation system", Microsystem Technologies, vol. 23, no. 8, pp3301-3309, 2017.
[4]N. F. Song, Q. Z. Cai, G. L. Yang, and H. L. Yin, "Analysis and calibration of the mounting errors between inertial measurement unit and turntable in dual-axis rotational inertial navigation system," Measurement Science and Technology, vol. 24, no. 11, pp. 115002, 2013.
[5]W. Sun, and Y. Gao, "Fiber-based rotary strapdown inertial navigation system," Optical Engineering, vol. 52, no. 7, pp. 076106-076106, 2013.
[6]X. Y. Wang, J. Wu, T. Xu, and W. Wang, "Analysis and verification of rotation modulation effects on inertial navigation system based on MEMS sensors," The Journal of Navigation, vol. 66, no. 5, pp. 751-772, 2013.
[7]A. Sugarbaker, S. M. Dickerson, J. M. Hogan, D. M. Johnson, and M. A. Kasevich, "Enhanced atom interferometer readout through the application of phase shear," Physical Review Letters, vol. 111, no. 11, pp. 510–516, 2013.
[8]F. Liu, W. Wang, L. Wang, and P. D. Feng, " Error analyses and calibration methods with accelerometers for optical angle encoders in rotational inertial navigation systems, " Applied Optics, vol. 52, no. 32, pp. 7724-7731, 2013.
[9]L. Kang, L. Y. Ye, K. C. Song, and Y. Zhou, "Attitude heading reference system using MEMS inertial sensors with dual-axis rotation," Sensors, vol. 14, no. 10, pp. 18075-18095, 2014.
[10]L. Wang, W. Wang, Q. Zhang, and P.Y. Gao, "Self-calibration method based on navigation in high-precision inertial navigation system with fiber optic gyro," Optical Engineering, vol. 53, no. 6, pp. 064103-064103, 2014.
[11]P.Y. Gao, K. Li, L. Wang, and Z.J. Liu, "A self-calibration method for tri-axis rotational inertial navigation system," Measurement Science and Technology, vol. 27, no. 11, pp. 115009, 2016.
[12]Z.H. Den, M. Sun, B. Wang, and M.Y. Fu, "Analysis and calibration of the non-orthogonal angle in duel-axis rotational INS," IEEE Transactions on Industrial Electronics, vol. 64, no. 6, pp. 4762-4771, 2017.
[13] P.Y. Gao, K. Li, L. Wang, and Z.J. Liu, "A self-calibration method for accelerometer nonlinearity errors in triaxis rotational inertial navigation system," IEEE Transactions on Instrumentation and Measurement, vol. 66, no. 2, pp. 243-253, 2017.
[14]B. Wang, Q. Ren, Z.H. Deng, and M.Y. Fu, "A self-calibration method for non-orthogonal angles between gimbals of rotational inertial navigation system," IEEE Transactions on Industrial Electronics, vol. 62, no. 4, pp. 2353-2362, 2015.
[15]S. O. Madgwick, A. J. Harrison, P. M. Sharkey, R. Vaidyanathan, and W. S. Harwin, "Measuring motion with kinematically redundant accelerometer arrays: theory, simulation and implementation," Mechatronics, vol. 23, no. 5, pp. 518–529, 2013.
[16]H. Liu, X. F. Wang, and Y. S. Zhong, "Quaternion-based robust attitude control for uncertain robotic quadrotors," IEEE Transactions on Industrial Informatics, vol.11, no.2, pp. 406-415, 2015.
[17]G. D. Feng, C. Y. Lai, and N. C. Kar, "Expectation-maximization particle-filter-and Kalman-filter-based permanent magnet temperature estimation for PMSM condition monitoring using high-frequency signal injection," IEEE Transactions on Industrial Informatics, vol. 13, no. 3, pp. 1261-1270, 2017.
[18]G. L. Du, P. Zhang, and X. Liu, "Markerless human–manipulator interface using leap motion with interval Kalman filter and improved particle filter," IEEE Transactions on Industrial Informatics, vol. 12, no. 2, pp. 694-704, 2016.
[19]G. Fedele, and A. Ferrise, "A frequency-locked-loop filter for biased multi-sinusoidal estimation," IEEE Transactions on Signal Processing, vol. 62, no. 5, pp. 1125-1134, 2014.
[20]H. K. Garg, and A. K. Kohli, "EEG spike detection technique using output correlation method: A Kalman filtering approach," Circuits, Systems, and Signal Processing, vol. 34, no. 8, pp. 2643-2665, 2015.
[21]M. S. Reza, and V. G. Agelidis, "A demodulation-based technique for robust estimation of single-phase grid voltage fundamental parameters," IEEE Transactions on Industrial Informatics, vol. 13, no. 1, pp. 166-175, 2017.
[22]J. B. Zhang, and H. C. Xu, "Microperturbation method for power system online model identification," IEEE Transactions on Industrial Informatics, vol. 12, no. 3, pp. 1055-1063, 2016.
[23]M. Vazquez-Olguin, Y.S. Shmaliy, and O.G. Ibarra-Manzano, "Distributed unbiased FIR filtering with average consensus on measurements for WSNs," IEEE Transactions on Industrial Informatics, vol. 13, no. 3, pp. 1440-1447, 2017.
[24]Z. H. Chen, Q. C. Zhu, and Y. C. Soh, "Smartphone inertial sensor-based indoor localization and tracking with iBeacon corrections," IEEE Transactions on Industrial Informatics, vol. 12, no. 4, pp. 1540-1549, 2016.
[25]S. Golestan, M. Ramezani, J. M. Guerrero, F. D. Freijedo, and M. Monfared, "Moving average filter based phase-locked loops: performance analysis and design guidelines," IEEE Trans Power Electron, vol. 29, no. 6, pp. 2750–2763, 2014.
[26]D. M. Dumont, K. M. Walsh, and B. C. Byram, "Improving displacement signal-to-noise ratio for low-signal radiation force elasticity imaging using bayesian techniques," Ultrasound in Medicine and Biology, vol. 42, no. 8, pp. 1986-1997, 2016.
[27]P.D. Hu, and C. N. Huang, "Shipborne high-accuracy heading determination method using INS-and GPS-based heading determination system," GPS Solutions, vol. 21, no. 3, pp. 1059- 1068, 2017.
[28]Z. Y. Gao, "Inertial navigation system technology," Beijing: Tsinghua university press, pp. 453, 2012. (in Chinese)
[29]K. R. Britting, "Inertial navigation system analysis," Wiley-Interscience, pp. 109–152, 1971.
[30]R. Jiang, G. L. Yang, R. Zou, J. Wang, and J. Li, "Accurate compensation of attitude angle error in a dual -axis rotation inertial navigation system," Sensors, vol. 17, no. 3, pp. 1-17, 2017.
[31]Z. Yao, and M. Q. Lu, "Signal multiplexing techniques for GNSS: The principle, progress, and challenges within a uniform framework," IEEE Signal Processing Magazine, vol. 34, no, 5, pp.16-26, 2017.
[32]P.D. Hu, S.Y. Wang, R. Zhang, X.X. Liu, and B. Xu, "Fast heading-rotation-based high-accuracy misalignment angle estimation method for INS and GNSS," Measurement, vol. 102, pp. 208-213, 2017.

Peida Hu received a B.E. in Mechanical Design and Automation from China University of Geosciences (Beijing) in 2003, a M.S. in Mechanical Design and Automation from Beijing Institute of Technology in 2006, and the Ph.D. in Instruments Science and Technology from Tsinghua University in 2011, China.

He is currently an associate professor at Tsinghua University, Beijing. His research interests include attitude determination, attitude evaluation and parameter identification for inertial navigation system and GNSS.

Bingxu Chen is an undergraduate student in Tsinghua University. He has been majoring in Measurement, Control Technology and Instruments in Tsinghua University, Beijing. His research interests include machine vision and parameter identification.

Chenxi Zhang is an undergraduate student in Tsinghua University. She has been majoring in Measurement, Control Technology and Instruments in Tsinghua University, Beijing. Her research interest is focus on parameter identification using Kalman filter and correlation method

Qiuping Wu received the B.S., M.S., and Ph.D. degrees in precision instrumentation from Southeast University, Nanjing, China, in 1994, 1997, and 2000, respectively.
From 2000 to 2002, he was a Post-Doctoral Scholar with the Department of Precision Instrument, Tsinghua University, Beijing, China, where he is currently an associate professor. His research interests include inertial sensors, integrated navigation, and gravity gradiometers.